# Polarimetric Passive Remote Sensing

Prof. J.A. Kong
Massachusetts Institute of Technology
Room 26-305
77 Massachusetts Avenue
Cambridge, MA 02139
phone: 617 253-8535 fax: 617 258-8525 email: kong@ewt.mit.edu

T.M. Grzegorczyk, Y. Zhang, C.O. Ao and B.-I. Wu
Massachusetts Institute of Technology
Room 26-305
77 Massachusetts Avenue
Cambridge, MA 02139
phone: 617 253-0986 fax: 617 253-0987 email: tomasz@ewt.mit.edu

Award Number: N00014-99-1-0175

## 1 OBJECTIVES

We seek to understand and predict the evolution of the brightness temperature (four Stokes parameters) of wind-driven foam-covered ocean surfaces. The correlation of polarimetric variation is studied as function of the medium state, modeled as a rough surface (ocean) overlayed by a random medium (foam).

Many independent results are obtain by using a wide variety of electromagnetic techniques, such as radiative transfer, integral equation, finite-difference time-domain, etc. Depending on the technique chosen, the foam coverage is modeled as either a dense medium composed of densely packed scatterers, a dielectric layer of non-uniform thickness or a succession of volumetric scatterers.

## 2 WORK COMPLETED

### 2.1 Dense medium radiative transfer theory for foam emission

The radiative transfer theory (RT) [1] has already been applied to the study of foam-covered ocean surfaces, often by modeling the foam as a layer of spherical air bubbles coated with a thin shell of sea water, overlaying the ocean surface. In the past, our approaches have considered both a foam layer much thicker than the penetration depth of the electromagnetic waves, and a layer constituted of small (compared to the electromagnetic wavelength) and sparsely distributed bubbles [2]. In the later case, a Rayleigh scattering theory has been used to obtain the extinction scattering properties of the foam layer, whereas in the former case, the small perturbation method of a plain ocean surface yielded a reflection matrix, further introduced in an iterative solution of the RT equations.

Recently, we have considered a more realistic model, taking into account the fact that over the actual wind driven ocean surface, the air bubbles are likely to be densely packed and present in a variety of sizes (including sizes large compared to the electromagnetic wavelength, thus rendering Rayleigh scattering theory invalid). To treat this more realistic situation, a dense medium radiative transfer (DMRT) theory has been studied [3, 4] and applied

# Report Documentation Page

*Form Approved*
*OMB No. 0704-0188*



| 1. REPORT DATE | 2. REPORT TYPE | 3. DATES COVERED |
|---|---|---|
| **30 SEP 2001** | | **00-00-2001 to 00-00-2001** |

| 4. TITLE AND SUBTITLE | 5a. CONTRACT NUMBER |
|---|---|
| **Polarimetric Passive Remote Sensing** | 5b. GRANT NUMBER |
| | 5c. PROGRAM ELEMENT NUMBER |
| 6. AUTHOR(S) | 5d. PROJECT NUMBER |
| | 5e. TASK NUMBER |
| | 5f. WORK UNIT NUMBER |
| 7. PERFORMING ORGANIZATION NAME(S) AND ADDRESS(ES) **Massachusetts Institute of Technology,,Room 26-305,77 Massachusetts Avenue,,Cambridge,,MA, 02139** | 8. PERFORMING ORGANIZATION REPORT NUMBER |
| 9. SPONSORING/MONITORING AGENCY NAME(S) AND ADDRESS(ES) | 10. SPONSOR/MONITOR'S ACRONYM(S) |
| | 11. SPONSOR/MONITOR'S REPORT NUMBER(S) |

12. DISTRIBUTION/AVAILABILITY STATEMENT
**Approved for public release; distribution unlimited**

13. SUPPLEMENTARY NOTES

14. ABSTRACT

15. SUBJECT TERMS

| 16. SECURITY CLASSIFICATION OF: | | | 17. LIMITATION OF ABSTRACT | 18. NUMBER OF PAGES | 19a. NAME OF RESPONSIBLE PERSON |
|---|---|---|---|---|---|
| a. REPORT **unclassified** | b. ABSTRACT **unclassified** | c. THIS PAGE **unclassified** | **Same as Report (SAR)** | **9** | |

to the calculation of ocean foam emission. Using the T-matrix formulation of the quasi-crystalline approximation (QCA), we incorporate coherent multiple scattering effects among the bubbles in the computation of the absorption, scattering, and extinction coefficients. These coefficients are subsequently used as inputs for the RT calculations. The brightness temperature can then be obtained by numerically solving the DMRT equation [5].

The most significant results obtained are as follows:

- Fig. 1(a) depicts the normalized extinction coefficient for bubbles of radius 1 mm, fractional thickness 0.03 (ratio between the thickness of the sea water coating and the total radius), and fractional volume 0.2. It can be seen that the scattering coefficient is quite small, and absorption contributes to nearly all the extinction in the foam. This fact is quantified in Fig. 1(b), where the albedo is shown to be less than 1.2% over a large range of frequencies. For the sake of comparison, the independent scattering is also displayed, and it is clearly seen that it overestimates the scattering coefficient and underestimates the absorption coefficient (thus predicts a much larger albedo).

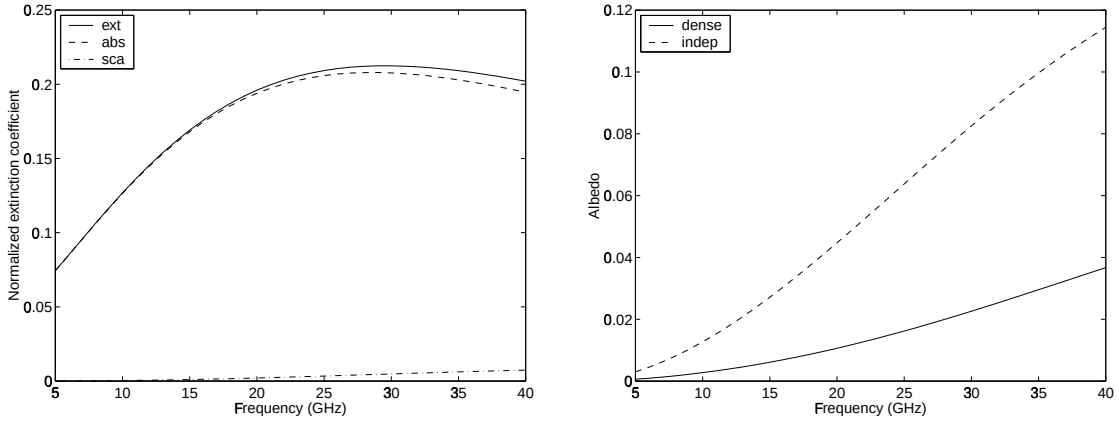


(a) Normalized extinction coefficient.

(b) Albedo.

***Figure 1: Extinction behavior of sea foam, where the bubbles have a radius of 1 mm and a fractional thickness of 0.03 (the fractional volume is 0.2).***

- Fig. 2 shows the brightness temperature at normal observation angle as a function of frequency. The vertical and horizontal polarizations have the same value due to azimuthal symmetry. The four cases illustrated correspond to two bubble radii ($a$ = 1 mm and 2 mm) and two bubble layer thicknesses ($d$ = 5 mm and 1 cm). The four curves show very similar frequency dependence, with thicker layer giving larger brightness temperature. The brightness temperature increases monotonously with frequency and appears to saturate at higher frequencies. Also shown for comparison are the brightness temperatures from the plain ocean surface and from Stogryn's empirical formula for foam emission [6].

- In the previous results, the foam emission has been calculated by assuming that the underlying ocean surface is flat. However, the actual wind-driven ocean surface contains multiscale roughnesses that can significantly affect the scattering and emission process. Hence, we have also taken into account the rough ocean surface partially by incorporating the geometric tilting effects of the large-scale ocean waves. Locally, we approximate the ocean surface by a tangent plane, and perform a coordinate transformation to retrieve the results in

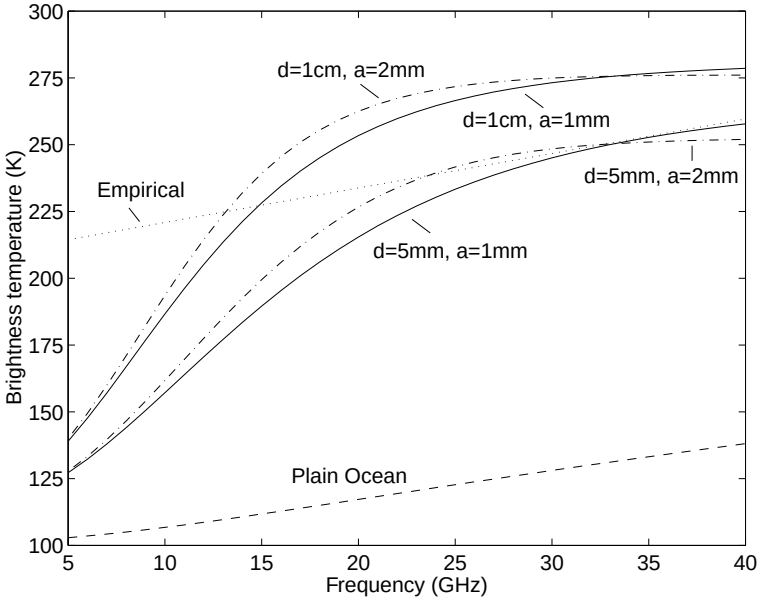


***Figure 2: Brightness temperature at nadir, as a function of frequency.***

the absolute system. In order to have a realistic model of ocean surface, the Cox-Munk [7] slope distribution for a wind-driven ocean surface has been used.

The ultimate results for the brightness temperature variations are depicted in Fig. 3. The amplitude of the azimuthal variations are small but measurable. Note that because of the upwind-downwind asymmetry in the Cox-Munk slope distribution, the brightness temperatures at $\phi = 0°$ and $\phi = 180°$ are not the same. The plain ocean has $U$ emission five times larger than that of the foam-covered ocean, which is because of the larger polarization difference of local emission. Yet, despite the difference in amplitude, the azimuthal dependence of the $U$ term for both cases are remarkably similar.

## 2.2 Integral equations compared to extended boundary conditions and finite-difference time-domain methods

In order not to have only an incoherent approach to study the brightness temperature of foam covered ocean surfaces, we have also made use of an integral equation (IE) approach. Our main concern in this work was to:

1. Be able to deal with very large ocean surfaces,

2. Study the impact of the foam coverage on the four Stokes parameters.

The first point led us to use a periodic Green's function in the IE kernel, allowing in this way the treatment of infinitely large surfaces. The second point has oriented our research toward a two-layer approach [8], thus modeling the rough ocean and its foam coverage as a half-space delimited by a periodic function $f_1$ of space, with a homogeneous dielectric layer delimited by the two functions $f_1$ and $f_2$. For the sake of generality, the two functions do not share any common restrictions, except to be defined over the same period. Notice that since $f_1$ can very well differ from $f_2$, they can be chosen such that $f_1$ models the ocean roughness (being possibly a random realization over the defined period), and $f_2 - f_1$ models the foam coverage, being a layer of inhomogeneous thickness (possibly negligible). For the specific situation of wind-driven ocean surface, $f_1$ can be constructed such

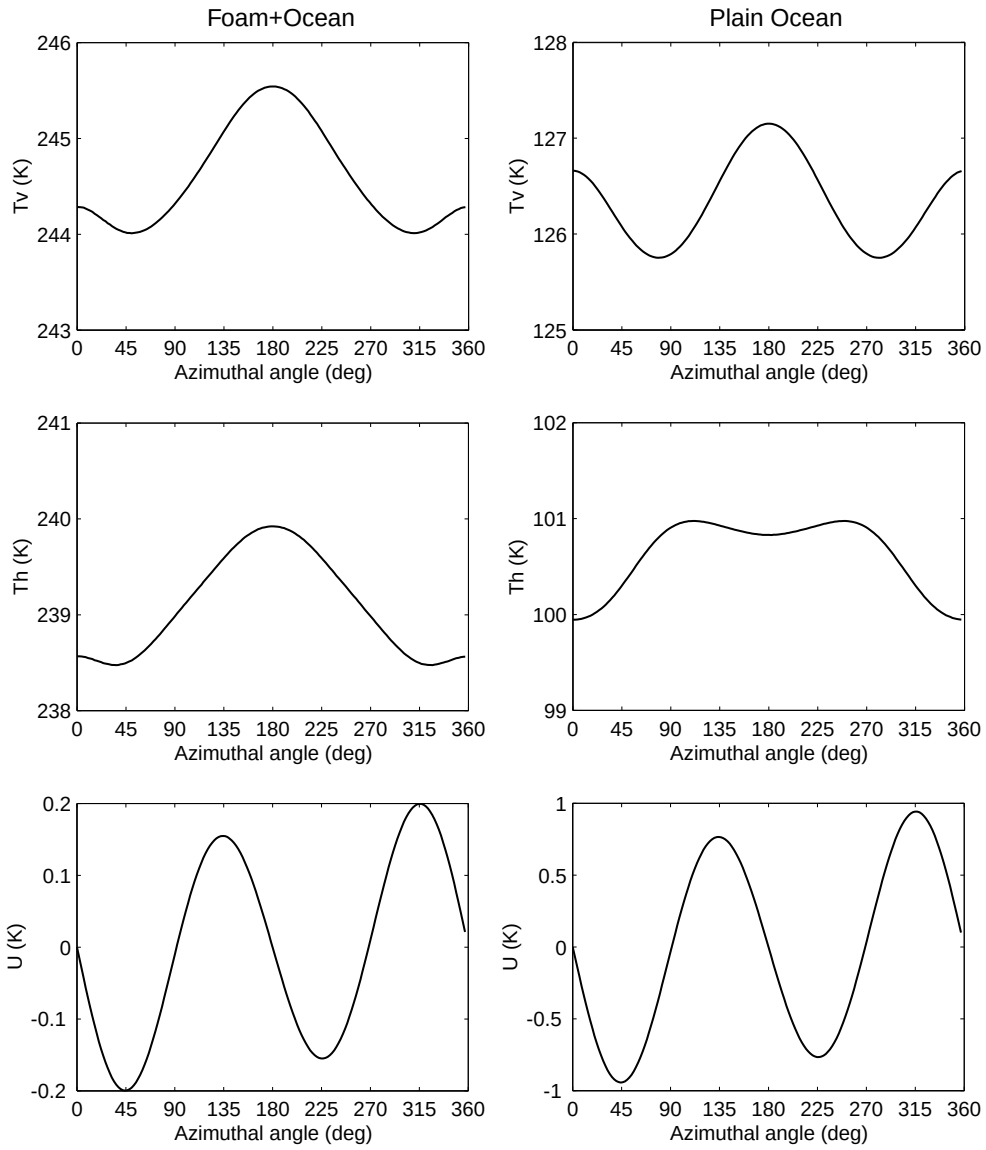


***Figure 3: Brightness temperature as function of azimuthal angle at*** $f = 19$ ***GHz.***

as to incorporate the two-scale model of the surface, the large-scale roughness being characterized by the Cox-Munk slope distribution, and the small-scale roughness characterized by the Durden-Vesecky power spectrum with hydrodynamic modulation.

The integral equation thus obtained has been solved by a standard Method of Moments (MoM) [9]. The results have been first compared to an existing Extended Boundary Conditions (EBC) method [10], capable of simulating similar conditions as those previously described, but with a limited range of surface rms heights. Yet, in the validity range of the EBC method, the MoM approach has proven to be very accurate, for both a one-layer ($f_2 = 0$) and two-layer ($f_2 \neq 0$) situations. The second test benchmark has been provided by published results [3], proving again the validity of the MoM approach.

In real situations, the wind-driven ocean surface has a very non uniform thickness of foam coverage and typically, young foam is more densely distributed on the leeward side of the waves, while old foam is more

uniformly distributed. In the two-layer approach, this forces to let $f_2 - f_1$ being small over large distances, which may yield numerical complications. In order to investigate this issue, we have studied the simple case of a sinusoidal ocean surface with a shifted-sinusoidal foam coverage. The distribution thus generated included a thick layer of foam on the downwind slope of the wave, and a very thin layer on the upwind slope (controlled by the shift of the function $f_2$). In this situation, we have studied the variation of the four Stokes parameters as a function of the shift, and have demonstrated a smooth variation, with no abnormal numerical behavior. We have also consistently verified that the first two Stokes parameters strongly vary with the foam coverage, while the $U$ term is much less sensitive, as illustrated in Fig. 4.

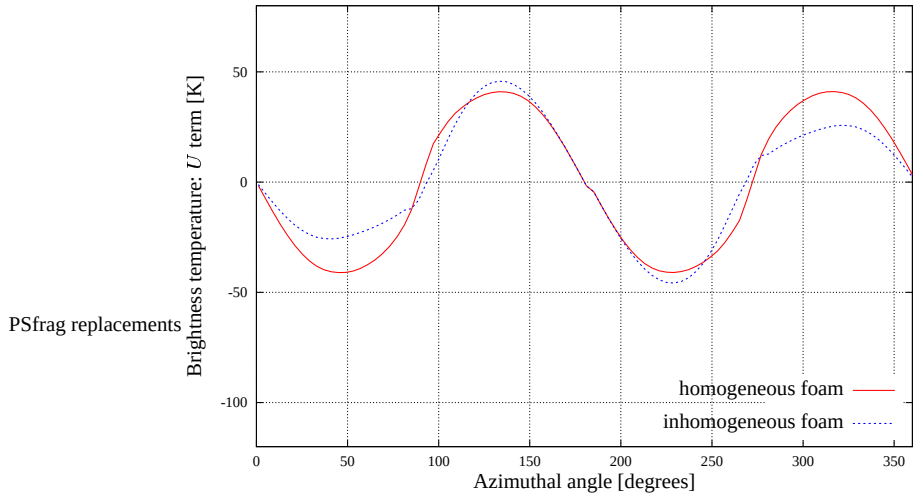


***Figure 4: Comparison between the $U$ term from a homogeneous and inhomogeneous layer of foam over a sinusoidal surface.***

Finally, for the sake of a more rigorous comparison, we have also implemented a two-layer finite-difference time-domain approach, which have shown to yield similar results to those obtained with the MoM for all four Stokes parameters. For the sake of illustration, we show in Fig. 5 the results for the first two Stokes parameters.

## 2.3 Electromagnetic interpretation of the third Stokes parameter ($U$ term)

Working directly on Maxwell's equations, it has been shown in the past that the first two Stokes parameters ($T_v$ and $T_h$) are even function of the angle between the wind direction and the look angle, whereas the last two Stokes parameters ($U$ and $V$) are odd functions of the same angle [11]. It has also been pointed out [12] that these two harmonics are reflecting two different properties of the medium: the first one accounts for the upwind and downwind asymmetry, while the second one for the upwind and crosswind asymmetry.

In this work, we have first considered the third Stokes parameter, and have tried to provide a physical interpretation for its variation in terms of the wind speed and the surface state. This first attempt for such an interpretation has been performed with a 1sc d model, where the ocean surface has been modeled as a succession of randomly distributed slopes (defined by an angle $\beta$). The second assumption was to use equivalent sources located on the rough surface, responsible for the radiation of the $U$ term. These sources have been modeled as Hertzian dipoles, with random orientation denoted by the angle $\alpha$.

Upon writing the electric field of a dipole source as function of a current moment function $\overline{f}(\theta, \phi)$ [13], and expressing the variations of $\overline{f}$ in terms of the angles $\alpha$ and $\beta$, we have obtained explicit expressions for the

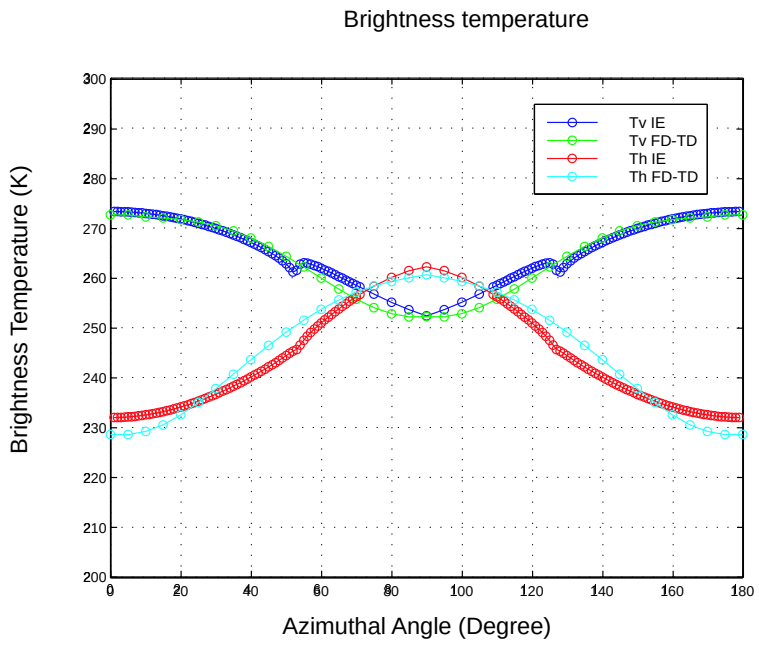


***Figure 5: Comparison between the rst two Stokes parameters predicted by and integral equation approach and the nite-difference time-domain approach***

horizontal and vertical components of the electric field ($\overline{E}_\theta$, $\overline{E}_\phi$) and hence, for the $U$ term as well. In order to take into account all dipole orientations, the results have been averaged with respect to $\alpha$, thus leaving the dependencies with the observation angles ($\theta$,$\phi$) and the surface tilting ($\beta$).

Various canonical situations have then been studied, like a saw-tooth surface profile with angles $\beta_1$ and $\beta_2$. These test cases have consistently shown that the $U$ term can be written as a superposition of two harmonics, like discussed in [11]. The first harmonic has shown to be associated with a $\sin\theta$ variation, while the second harmonic with a $\cos\theta$ variation. These conclusions have given a lots of insight and understanding of the variation of the $U$ term in terms of azimuthal ($\phi$) and polar ($\theta$) angles.

As an ultimate verification, we have compared these theoretical predictions with the measured WINDRAD data [14]. Both the two harmonic variations and the $\theta$ dependence have been verified, as can be seen by a direct inspection of Fig. 6.

The concluding statement issued from this theoretical study were as follows:

- The averages $< \sin 2\beta >$ and $< \sin^2 \beta >$ are non-negative, and related to wind speed,
- The dipole moment is related to the physical temperature and conductivity of sea water,
- The first harmonic of the $U$ term vanishes at normal looking angle ($\theta = 0°$),
- The coefficients and wind direction can be calculated by using multi-looking data.

# References

[1] L. Tsang, J. Kong, and K. Ding, *Scattering of Electromagnetic Waves: Theories and Applications*. Wiley, New York, 2000.

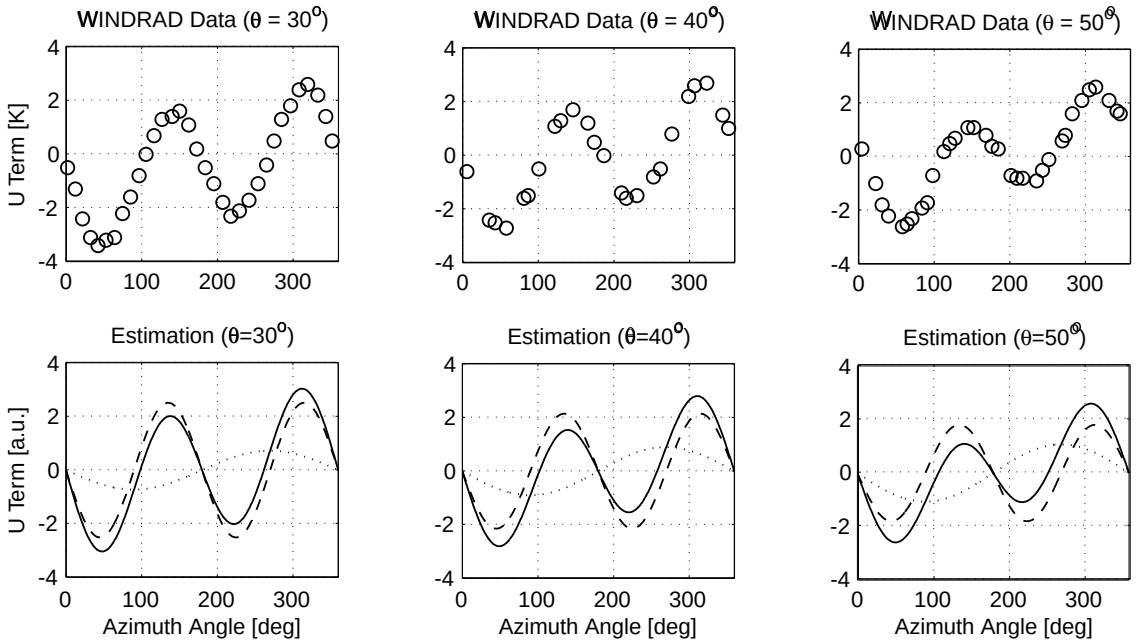


***Figure 6: Comparison between the theoretical model for the U term and the WINDRAD measured data.***


[2] Y. Zhang, *Forward and inverse problems in microwave remote sensing of objects in complex media*. PhD thesis, Massachusettes Institute of Technology, 2000.

[3] L. Tsang, J. Kong, K. Ding, and C. Ao, *Scattering of Electromagnetic Waves: Numerical Simulations*. Wiley, New York (in press), 2000.

[4] L. Tsang and J. Kong, *Scattering of Electromagnetic Waves: Advanced Topics*. Wiley, New York (in press), 2000.

[5] C. O. Ao, *Electromagnetic Wave Scattering by Discrete Random Media with Remote Sensing Applications*. PhD thesis, Massachusettes Institute of Technology, 2001.

[6] A. Stogryn, "The emissivity of sea foam at microwave frequencies," *J. Geophys. Res.*, vol. 77, pp. 1658–1666, March 1972.

[7] C. Cox and W. Munk, "Measurements of the roughness of the sea surface from photographs of the sun's glitter," *J. Opt. Soc. Am.*, vol. 44, pp. 838–850, November 1954.

[8] J. J. Johnson, J. A. Kong, R. T. Shin, D. H. Staelin, K. O' Neill, and A. Lohanick, "Third stokes parameter emission from a periodic water surface," *IEEE Trans. on Geosci. Remote Sens.*, vol. 31, pp. 1066–1080, September 1993.

[9] R. F. Harrington, *Field Computation by Moment Method*. IEEE Press, 1993. ISBN 0-7803-1014-4.

[10] S. Chuang and J. A. Kong, "Wave scattering from a periodic dielectric surface for a general angle of incidence," *Radio Sci.*, vol. 17, pp. 545–557, May-June 1982.

[11] S. Yueh, R. Kwok, and S. Nghiem, "Polarimetric scattering and emission properties of targets with reflection symmetry," *Radio Sci.*, vol. 29, pp. 1409–1420, Nov.-Dec. 1994.

[12] S. H. Yueh, “Modeling of wind direction signals in polarimetric sea surface brightness temperature,” *IEEE Trans. on Geosci. Remote Sens.*, vol. 35, pp. 1400–1418, June 1997.

[13] J. A. Kong, *Electromagnetic Wave Theory*. EMW, 2000. ISBN 0-9668143-9-8.

[14] S. Yueh, W. Wilson, F. Li, S. Nghiem, and W. Ricketts, “Polarirmetric measurements of sea surface brightness temperature using an aircraft K-band radiometer,” *IEEE Trans. on Geosci. Remote Sens.*, vol. 33, pp. 85–92, January 1995.